Decolorization efficiency of Methyl orange simulative wastewater by a reverse electrodialysis reactor: experiments and kinetic models

Qiang Leng, Shiming Xu*, Xi Wu, Sixue Wang, Debing Wu, Fujiang Dong, Dongxu Jin, Ping Wang

Key Laboratory of Ocean Energy Utilization and Energy Conservation of Ministry of Education, School of Energy and Power Engineering, Dalian University of Technology, Dalian 116024, Liaoning, China, Tel. +86 13050539216; email: xsming@dlut.edu.cn (S. Xu), Tel. +86 18941197912; emails: lqdllg@mail.dlut.edu.cn (Q. Leng), xiwu@dlut.edu.cn (X. Wu), wsx979997@mail.dlut.edu.cn (S. Wang), dbwu@mail.dlut.edu.cn (D. Wu), dongfj1991@163.com (F. Dong), dongxujin@dlut.edu.cn (D. Jin), wp2006@dlut.edu.cn (P. Wang)

ABSTRACT

A novel advanced oxidation process technology of dye wastewater with a reverse electrodialysis reactor was investigated experimentally in this paper. The influences of the operating conditions (concentration of Cl^- and Fe^{2+}, pH value, electrode rinse solution (ERS) and airflow rates, and current density) on the decolorization efficiencies of Methyl orange simulative wastewater were explored and discussed experimentally and theoretically. The results showed that the color of the wastewater in the anodic and cathodic degradation loops was effectively faded, and the decolorization efficiency was related to the operating conditions. The effects of Cl^- and Fe^{2+} concentrations on the decolorization efficiency were relatively slight. However, the effects of pH value, ERS and airflow rates and current density on the decolorization efficiency were relatively significant. A simple semi-empirical kinetic model based on Fermi's equation was applied to describe the wastewater oxidation process in two degradation loops. The apparent rate constants and the transition time in the model were obtained by experimental data. The results calculated by the model had a good fit for the experimental data of the anodic degradation loop. Meanwhile, the cathodic degradation loop model has been modified, and it had a good fit for the experimental data of the cathodic degradation loop. The fitting precisions of the model, R^2 values, are in the ranges of 0.96–0.99 for oxidation process under different operation parameters.

Keywords: Dye wastewater; Methyl orange; Decolorization efficiency; Reverse electrodialysis reactor; Kinetic model

1. Introduction

Printing and dyeing enterprises will discharge much dye wastewater and waste heat in their production processes. Since most dye wastewaters are resistant to treatment by conventional biological treatment technologies, various new wastewater treatment technologies with high efficiency and low cost have been developed to remove organic dyes in wastewaters over the past three decades [1–3]. Among these new technologies, the electrochemical advanced oxidation processes (EAOPs) have attracted increasing interest because of their immense potential. The EAOPs present several advantages for organic wastewater treatments [4,5]. They are (1) moderate requirements for temperature and pressure; (2) avoiding the risk of transportation and storage of auxiliary chemicals; (3) no secondary waste streams, (4) easy combination

---

* Corresponding author.

with other treatment technologies and (5) easy full-automatic control.

However, EAOPs need to consume huge amounts of additional power, limiting their development in industrial activities [6]. In recent years, a kind of heat engine called chemical heat engine (CHE) has attracted interest worldwide [7–9]. Low-grade heat (LGH) or waste heat is first converted into salinity gradient energy (SGE) of working fluids by thermal separation or decomposition, and then the SGE is converted into electrical energy by reverse electrodialysis (RED) stacks. By utilizing redox reactions at two electrodes of reverse electrodialysis reactors (REDRs), chemical heat engine technology can be introduced to treat the organic or inorganic wastewaters to achieve the objective of 'waste-heat to treat wastewater' [10–12]. The 'waste-heat to treat wastewater' technology has the large prospect of lower energy consumption, more environmental friendliness, and lower wastewater treatment costs.

Like the CHE, the cycle of 'waste-heat to treat wastewater' also has two energy conversion processes. The first energy conversion process is the conversion of waste-heat to SGE by thermal separation or decomposition technologies. The technologies involved relative technologies in this process are relatively mature, especially thermal separation technologies such as multi-effect distillation (MED), multi-stage flash distillation (MSFD) and membrane distillation (MD), which have been widely applied in practical engineering [13–15]. The second energy conversion process is the conversion of SGE to wastewater treatment energy by REDRs. Nevertheless, the technologies involved in this process are immature. Only a few pieces of literature about the technology of wastewater treatment by REDRs have been openly published.

Scialdone et al. [16] first proposed a new approach for the simultaneous generation of electric energy and treating wastewater contaminated by Cr(VI) by a RED stack. The results showed that Cr(VI), a very toxic compound, in wastewater was removed successfully by a reduction reaction at the carbon cathodic electrode of the stack. The addition of Cr(VI) to the cathodic solution would enhance the stack's power output. Later, the authors conducted another approach to simultaneously generate electric energy and azo dye (Acid Orange 7, AO7) wastewater treatment by a REDR with 40–60 cell pairs [17]. The results showed that the reactor could perform various electrochemical approaches (electro-Fenton, electro generation of active chlorine and coupled process) to oxidate and degrade organic pollutants in wastewater under the action of SGE.

Zhou et al. [18] reported the treatment of ammonia nitrogen simulative wastewater by REDR. The results showed that in the electrode rinse solution (ERS) with chloride salts, active chlorine was generated in the anodic channel to degrade the ammonia nitrogen in wastewater. The maximum ammonia nitrogen removal efficiency and output power density were 98% and 0.06 W m^{-2} under ERS and working fluids flow rate of 250 and 50 mL min^{-1}, respectively.

Xu et al. [10,11] also reported the degradation mechanism of organic dye wastewater by REDRs. The effects of different degradation modes on the decolorization efficiencies of azo dye (AO7) simulative wastewater were explored experimentally [10]. The results showed that after 20 min of treatment, the decolorization efficiencies of AO7 simulative wastewater for the independent degradation mode reached 99.93% and 96.52% in the anodic and cathodic degradation loops, respectively, while that for the synergetic degradation mode only reached 82.85%. Later, the authors investigated the influence of the output current on the decolorization efficiency of AO7 similative wastewater by a multi-stage REDR series system [11]. The results showed that the series system could effectively fade the color of AO7 simulative wastewater and output a certain amount of electric energy simultaneously. When the current was 0.1 Å, the system's overall performances were relatively optimal under the given experimental conditions. The number of reactors, total decolorization rate, utilization efficiencies of SGE and membrane area, and net output power reached 19, 1.91 mg s^{-1}, 6.92 mg J^{-1}, 31.21 mg m^{-2} s^{-1} and 0.68 W, respectively.

Although the reports above demonstrate the excellent removal effect of organic or inorganic pollutants in wastewater by REDRs, the research on wastewater treated by REDR is insufficient, especially for theoretical research. Methyl orange (MO), as an azo compound, is usually used as a coloring agent in many application fields. It is resistant to biological treatment but can be oxidized and degraded by REDR powered by SGE. In this work, the decolorization effect of the operation parameters of REDR on the Methyl orange (MO) dye simulative wastewater will be investigated and analyzed through experiment firstly. And then, a kinetic model with a single function based on Fermi's equation will be proposed, which aims to describe the transient dye concentration data in this complex process.

2. Materials and method

2.1. Experimental system

The experimental system of MO simulative wastewater treatment with a REDR powered by SGE is shown in Fig. 1. The structure and working principle of REDR were introduced in our previous works in detail [10,11] so that they are described briefly here.

As shown in Fig. 1, a REDR comprises two endplates, two electrodes (anode and cathode), a certain amount of alternative arrangement of anion and cation exchange membranes (AEMs and CEMs) and woven spacers to separate the ion-exchange membranes (IEMs). When the low concentration (LC) and high concentration (HC) salt solutions (working fluids) flow simultaneously through their corresponding channels separated by IEMs and woven spacers, the anions and cations in the HC will immigrate across IEMs toward the LC under the action of salinity gradient. Therefore, an ion current in REDR is created, which leads to a membrane electric potential generation. The theoretical electric potential (OCV) of a REDR with N membrane pairs can be calculated by the Nernst equation [19].
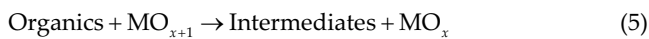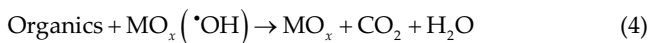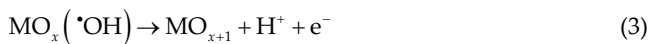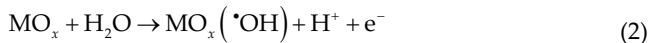
$$OCV = \left(\alpha_{CEM} + \alpha_{AEM}\right)\frac{NRT}{zF}\ln\left(\frac{\gamma_c x_c}{\gamma_d x_d}\right) \tag{1}$$

where α is permselectivity of IEMs; R is the universal gas constant, 8.314 J mol^{-1} K^{-1}; T is temperature, K; z is ion valence
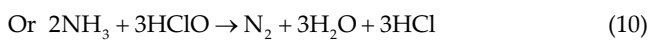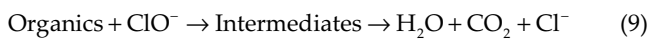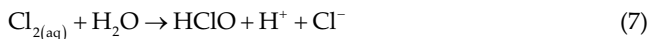
of electrolyte in working fluids; F is Faraday constant, 96,485 C mol⁻¹; γ is activity coefficient; x is concentration, mol L⁻¹. Subscripts: d and c denote concentrated and diluted solutions, respectively; AEM and CEM denote anion and cation exchange membranes, respectively.

At the membrane potential action, a redox reaction will be created at two electrodes of REDR, and the electrons produced by the redox action transport from the anode to the cathode through the external circuit to form a current and output power. When organic or inorganic wastewater flows through the anodic or cathodic channels of REDR, several electrochemical oxidation or reduction processes will have occurred. Two types of oxidation processes, direct and indirect oxidations, will occur. The reaction equations are:
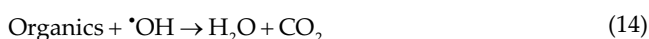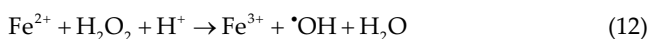
Direct oxidation process [20,21]:

$$MO_x + H_2O \rightarrow MO_x\left(\text{}^\bullet OH\right) + H^+ + e^- \tag{2}$$

$$MO_x\left(\text{}^\bullet OH\right) \rightarrow MO_{x+1} + H^+ + e^- \tag{3}$$

$$Organics + MO_x\left(\text{}^\bullet OH\right) \rightarrow MO_x + CO_2 + H_2O \tag{4}$$

$$Organics + MO_{x+1} \rightarrow Intermediates + MO_x \tag{5}$$

Indirect oxidation process [5,22]:

$$2Cl^- \rightarrow Cl_{2(aq)} + 2e^- \tag{6}$$

$$Cl_{2(aq)} + H_2O \rightarrow HClO + H^+ + Cl^- \tag{7}$$

$$HClO \leftrightarrow H^+ + ClO^- \tag{8}$$

$$Organics + ClO^- \rightarrow Intermediates \rightarrow H_2O + CO_2 + Cl^- \tag{9}$$

$$Or \ 2NH_3 + 3HClO \rightarrow N_2 + 3H_2O + 3HCl \tag{10}$$

Similarly, when a gas diffusion electrode is used as the cathode, both organic wastewater as a cathodic rinse solution (CES) and airflow through the cathodic channel of REDR, and a cathodic oxidative reaction called electro-Fenton (EF) reaction will be created [23,24]. The reaction equations are:

$$O_2 + 2H^+ + 2e^- \rightarrow H_2O_2 \tag{11}$$

$$Fe^{2+} + H_2O_2 + H^+ \rightarrow Fe^{3+} + \text{}^\bullet OH + H_2O \tag{12}$$

$$Fe^{3+} + e^- \rightarrow Fe^{2+} \tag{13}$$

$$Organics + \text{}^\bullet OH \rightarrow H_2O + CO_2 \tag{14}$$

Obviously, when wastewater flows through either anodic or cathodic channels of the REDR, organic or inorganic pollutants in wastewater can be removed by oxidation and degradation reactions. There are two wastewater treatment modes by REDR: anodic and cathodic independent and synergetic degradation modes. In this work, anodic and cathodic independent degradation mode is chosen to avoid the interaction of oxidants generated at the anode and cathode in synergetic degradation mode [10]. As shown in Fig. 1, there are two degradation loops in the independent degradation mode, and the wastewater can be treated in each loop independently.

2.2. Reverse electrodialysis reactor

The lab-scale REDR with 40 membrane pairs is the same as our previous study [10,11], and it is homemade. The specification and materials of the REDR are listed in Table 1. A titanium plate coated with ruthenium and iridium dioxides (Ti/RuO₂-IrO₂) was used as the anode, and its size was 130 mm × 70 mm × 1 mm (length × width × thickness). A gas diffusion electrode, carbon felt with a porosity of 75%, was used as the cathode and its size was 115 × 70 × 5 mm. A bubble generator is set below the carbon felt cathode to form tiny air bubbles in the CRS flowing cathodic channel. Accordingly, the length of the cathode is shorter than that of the anode. The effective length of IEMs equals that of an anode. The thicknesses of the anodic and cathodic channels are 3 mm and 5 mm, respectively. The main IEMs in the reactor are Selemion type IEMs made by AGC Company. Two AEMs made by Fujifilm Company were used to separate the working fluids and ERS was used to form the electrode channels. The working fluids (LC and HC) and ERS flow along the length of electrodes from bottom to top.

2.3. Working fluids and ERS

Aqueous NaCl solutions were used as the working fluids, LC and HC, and their initial concentrations were 3 and 0.03 mol kg⁻¹, respectively. Each volume of the LC and HC was 1 L. The LC and HC were pushed respectively by two large peristaltic pumps (Longer BT600-2J) to flow through the reactor at the same flow rate of 82 mL min⁻¹ (mean velocity on the membrane surface of 0.2 cm s⁻¹).

An azo dye, Methyl orange (MO), is used as a degradation object, and its characteristics are listed in Table 2. Total 1 L of MO simulative wastewater with MO concentration of 100 mg L⁻¹ was prepared artificially. Each 0.5 L of wastewater is used as the ARS or CRS and charged into its corresponding tank, as shown in Fig. 1. The supporting electrolyte in ARS is sodium chloride (NaCl) for the anodic oxidation process, and the catalyst in CRS is ferrous sulfate (FeSO₄) for the EF reaction. The pH value of CRS is adjusted by adding diluted sulfuric acid (H₂SO₄). The ARS and CRS are pushed respectively by two small peristaltic pumps (Karmor) to flow circularly in the anodic and cathodic degradation loops between the reactor and their storage tanks.

All electrolytes and MO that are used to prepare HC, LC and ERS are provided by Damao Chemical Reagent Factory (China), and their purities are higher than 99.8%. The solvent is deionized water.
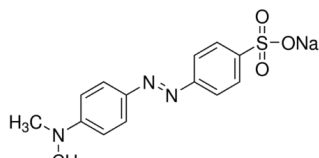
Table 1
Parameters of REDR, IEMs and woven spacer

Items	Parameters		Symbol	Unit	Value
	Membrane pairs		N	–	40
Profile of REDR	Width		–	mm	150
	Length		–	mm	250
IEM* (Asahi Glass Company)	Permselectivity[a]	CEM	α_{CEM}	–	0.96
		AEM	α_{AEM}	–	0.96
	Area resistance[b]	CEM	R_{CEM}	Ω cm^{-2}	3
		AEM	R_{AEM}	Ω cm^{-2}	2.8
	Membrane thickness		δ_m	mm	0.12
AEM* (Fujifilm Company)	Permselectivity[a]		α_{AEM}	–	0.96
	Area resistance[b]		R_{AEM}	Ω cm^{-2}	1.6
	Membrane thickness		δ_m	mm	0.16
	Thickness		δ	mm	0.35
Woven spacer	Aperture ratio		–	%	50
	Shading coefficients		f	–	1.8
	Blockage coefficients		β	–	0.5

*Data provided by the manufacturer;
[a]Measured in 0.1 M/0.5 M NaCl solutions at 25°C;
[b]Measured in 0.5 M NaCl solutions at 25°C.

Table 2
Characteristics of Methyl orange

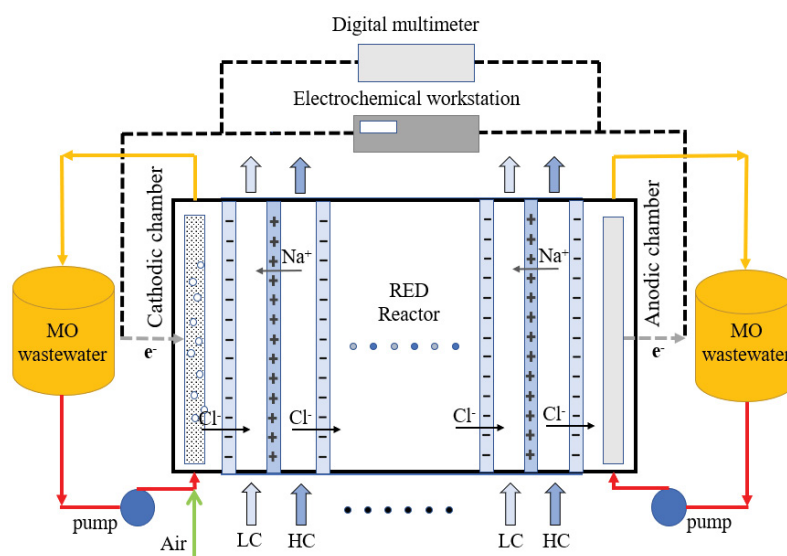| Molecular Formula	Molecular structure	Molecular weight (g mol^{-1})	Peak absorption wavelength (nm)	Color Index (C. I. No.)
C$_{14}$H$_{14}$N$_3$SO$_3$Na		327.33	508	13025

Fig. 1. The structure and working principle of REDR.

2.4. Instruments and analytical procedures

The specification and characteristics of the test instruments used in this investigation are listed in Table 3. A UV-Vis Spectrophotometer (Shimadzu UV1780) was used to measure the absorbance of MO in the wastewater at its peak absorption wavelength of 508 nm. The equation of the calibration curve for MO by experiments is (Degree of association, $R^2 = 0.9987$),

$$y_{MO} = 0.122824 x_{MO} \tag{15}$$

where y_{MO} is the value of absorbance at the peak absorption wavelength of MO; x_{MO} is the concentration of MO in the wastewater, mg L^{-1}.

The decolorization efficiency of MO simulative wastewater (η_{de}) can be calculated using the following equation.

$$\eta_{de} = \left(1 - \frac{C_t}{C_0}\right) \times 100\% \tag{16}$$

where C_0 is the initial concentration of MO in the simulative wastewater, mg L^{-1}; C_t is the concentration of MO in the simulative wastewater after treating t time.

An electrochemical workstation listed in Table 3 is employed to provide the REDR with a constant reverse current. Moreover, a conductivity meter and electronic scales are used to prepare aqueous NaCl solutions and ERSs. A pH meter was used to detect the pH value of CRS during the experiments.

In this work, Fermi's function, a single semi-empirical function, is introduced to fit the experimental data. The function represented by Eq. (17) was developed earlier and used to explain the history of organic pollutant concentration in wastewater [25,26]. The Marquardt–Levenberg algorithm finds the coefficients (parameters k, t^*) and gives the best fit between the experimental and model data.

$$\frac{C}{C_0} = \frac{1}{1 + \exp\left[k(t - t^*)\right]} \tag{17}$$

where k is an apparent reaction rate constant, min^{-1}; t^* is a transition time that determines the inflection point of the concentration curve (the location of which determines the inflection point of the concentration curve).

2.5. Operation parameters and current density

Since the variations of current density and ERS operation parameters such as the concentration of supporting electrolyte, ERS flow rate, pH value and airflow rate will affect the decolorization efficiency of the wastewater treated by REDR, the variation ranges of these parameters are set as listed in Table 4 during experiments. Here, the current density is defined as the output current per unit anodic area, A m^{-2}.

3. Results and discussion

3.1. Anodic degradation loop

Since the electrons produced by the redox reaction at two electrodes of REDR are transported by the external circuit from the anode to the cathode, the reactions between the anode and cathode are correlated. The operation parameters of the cathodic degradation loop and the current density are unchanged while exploring the influence of ARS operation parameter variations on the decolorization efficiencies of the wastewater in the anodic degradation loop. The CRS flow rate, ferrous ion concentration, pH value and airflow rate of the cathodic degradation loop were 128 mL min^{-1}, 1.5 mM, 2 and 600 mL min^{-1}, respectively. Moreover, the current density was 3.10 A m^{-2}.

3.1.1. Effect of chlorine salt concentration (Cl$^-$)

According to Eqs. (6)–(10), the indirect oxidation process will take place when chloride ions (Cl$^-$) exist in ARS. Therefore, the chlorine salt concentration in wastewater plays an important role in the anodic oxidation process. The influence of chlorine salt concentration on the decolorization efficiency of MO simulative wastewater is shown in Fig. 2.

Fig. 2 shows that when the chloride concentration in the wastewater increases from 0.05 to 0.5 M, the decolorization efficiency of the wastewater rises from 79.63% to 95.83% after treatment for 8 min. However, when the treatment time extends to 16 min, the decolorization efficiency can almost reach 100%, regardless of whether the chloride concentration in the wastewater changes. This means that the direct oxidation reaction plays the main role in the decolorization of wastewater and the indirect oxidation reaction only plays a role in promoting decolorization. Moreover, increasing the concentration of Cl$^-$ can enhance the decolorization efficiency due to more active

Table 3
Specification and characteristics of the test instruments used in the experimental system

Equipment	Brand	Model number	Precision
Conductivity Meter	Mettler Toledo	FiveEasy Plus + InLab® 710	±0.5%μs cm^{-1}
Electrochemical Workstation	CH Instruments	CHI660E+CHI680C	0.1 mV
UV-Vis Spectrophotometer	Shimadzu	UV1780	±0.002
Electronic scales	Ohaus	CP153C	0.001 g
pH meter	LI CHEN	pH-100A/100	±0.2 pH

Table 4
Variation ranges of ERS operation parameters and output current of REDR

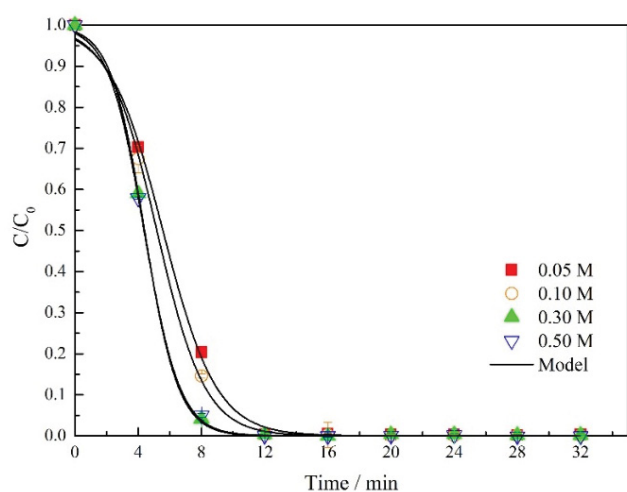|	ARS	CRS
Initial concentration of MO (mg L^{-1})	100	100
Flow rate (mL min^{-1})	32–128	32–128
NaCl (M)	0.05–0.50	–
Fe$_2$Cl (mM)	–	0.1–1.5
pH	–	1.5–3.5
Airflow rate (mL min^{-1})	–	600–1,200
Current density (A m^{-2})	0.62–3.1	

Fig. 2. Effect of chloride concentration on decolorization efficiency of MO simulative wastewater in the anodic degradation loop (Operation conditions: ARS flow rate: 82 mL min^{-1}). Curves connecting the points are fitted by Eq. (17), and the coefficients are given in Table 5.

chlorine species generated in the anodic compartment. It can also be seen from the figure that when the wastewater is fully faded, the treatment time is 12 or 16 min for chloride concentrations of 0.3 or 0.05 M. This further proves that chloride has promoting action for the wastewater decolorization. The experimental results also show that when the chloride concentration in the wastewater is more than 0.3 M, the increase of chloride concentration has almost no effect on the decolorization efficiency. The reason is that the reaction process of active chlorine species is switched to under current control from under mass transport control when the concentration of Cl^{-1} surpasses 0.3 M. Therefore, there are few promotions for degradation effect when Cl$^-$ exceeds 0.3 M.

3.1.2. Effect of ARS flow rate

Fig. 3 demonstrates the effect of the ERS flow rate on the decolorization efficiency of MO simulative wastewater. It can be seen from the figure that the decolorization efficiency rises with increasing ERS flow rate. After treatment
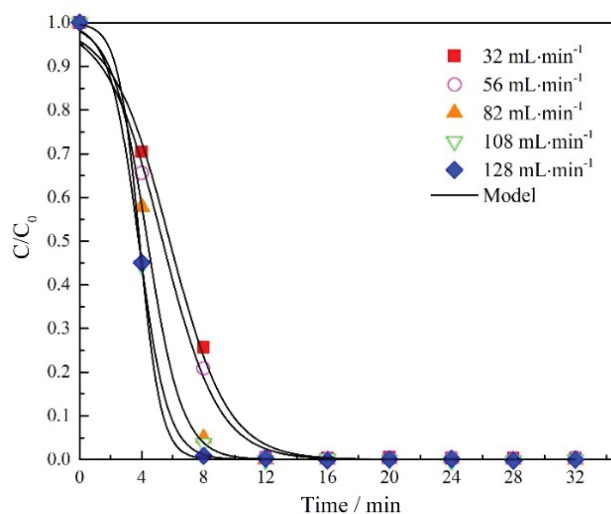

Fig. 3. Effect of ARS flow rate on the decolorization efficiency of MO simulative wastewater in the anodic degradation loop (Operation conditions: chloride concentration: 0.5 M). Curves connecting the points are fitted by Eq. (17), and the coefficients are given in Table 5.

for 8 min, the decolorization efficiency rises from 74.34% to 99.15% when the ARS flow rate increases from 32 to 128 mL min^{-1}. However, when the treatment time extends to 16 min, the decolorization efficiency can almost reach 100%, regardless of the flow rate changes. This means that an increase in the ARS flow rate can shorten the decolorization time of wastewater. Suppose the decolorization efficiency is set as 99%. In that case, the decolorization time of the wastewater can shorten from 16 to 8 min when the flow rate rises from 32 to 128 mL min^{-1}, which means that the energy consumption of the wastewater treatment can be reduced by half.

In fact, the oxidative degradation process of organic matter in wastewater at an electrode channel of REDR is a mass transfer process. When the ERS flow rate increases, the concentration polarization on electrode surfaces will be improved. The oxidants generated on electrode surfaces diffuse easily from the electrode surfaces to the mainstream area. This leads to the mass transfer coefficients between organic wastewater and electrode surfaces rising and the degradation rate of organic matter in wastewater increasing [27]. With the extension of treatment time, the concentrations of organic matter in the wastewater decrease gradually. This leads to a decrease in the mass transfer force or the current efficiency of the degradation reaction process. As a result, the decolorization efficiency of the wastewater tended to be the same when the treatment time was extended to 16 min, regardless of whether the ARS flow rate changed.

Table 5 lists all experimental conditions of the anodic degradation loop and the obtained kinetic parameters after the regression of MO concentration histories in the wastewater. It can be seen from the table or the two figures shown above that there is a better fit precision between the experimental data and the calculated data by Eq. (17).

3.2. Cathodic degradation loop

Similarly, to avoid interference between anodic and cathodic reactions, the operation parameters of the anodic degradation loop and the current density are unchanged while exploring the influence of CRS operation parameter variations on the decolorization efficiencies of the wastewater in the cathodic degradation loop. The ARS flow rate and chlorine salt concentration were 0.5 M and 128 mL min^{-1}, respectively, and the current density was 3.10 A m^{-2}.

3.2.1. Effect of ferrous ion concentration (Fe^{2+})

The ferrous ion Fe^{2+} is a catalyst in the electro-Fenton process and plays an important role in Eq. (12) to produce a strong oxidant (hydroxyl radical). Fig. 4 indicates the effect of the Fe^{2+} concentration in the wastewater on the decolorization efficiency of the wastewater. It can be seen from the figure that the decolorization efficiency will change with the variations of Fe^{2+} concentration at the same treatment time. After treatment for 20 min, the decolorization efficiencies were 91.71%, 98.21% and 95.15% when the Fe^{2+} concentrations were 0.1, 1 and 1.5 mM, respectively. The results indicate that microscale ferrous ions can effectively maintain the EF reaction procedure in wastewater. This is because Fe^{3+} ions can be translated to Fe^{2+} ions continually by Eq. 13 to maintain the concentration of Fe^{2+} keep steady.

However, the results also show that an excessively high ferrous ion concentration is not good for decolorization efficiency in the experimental range. The reason is that at the variation range of a certain ferrous ion concentration, the increase of Fe^{2+} concentration can promote EF reaction to produce more hydroxyl radical ($^{\bullet}$OH) from H$_2$O$_2$, which improves the decolorization efficiency of the wastewater in the cathodic degradation loop. However, when the Fe^{2+} concentration in the wastewater exceeds 1.0 mM, the excessive iron ions (Fe^{2+}, Fe^{3+}, FeOH$^+$) have an adverse reaction with various free radicals ($^{\bullet}$OH, HO$_2^{\bullet}$, etc.) produced at the cathode reaction to affect the decolorization efficiency [6]. The decolorization efficiency of the wastewater in the cathodic degradation loop starts to show a downward trend. Therefore, when the ferrous ion concentration in the wastewater is 1.0 mM, there is a relatively high decolorization efficiency in the cathodic degradation loop.

3.2.2. Effect of pH value

It is well known that EF reaction must be performed under acidic condition [28–30]. However, the pH value of wastewater will significantly affect the EF reaction in the cathodic channel of REDR. Fig. 5 illustrates the effect of the pH value on the decolorization efficiency of the wastewater.

It can be seen from Fig. 5 that the decolorization efficiencies present a variation trend of first increasing and then decreasing as the pH value of the wastewater rises from 1.5 to 3.5 at the same treatment time. The main reasons why the pH value variations of the wastewater affect the decolorization efficiency are as follows:

• A high pH value means a low H$^+$ concentration in the wastewater, which is adverse to the formation of H$_2$O$_2$ by a reduction reaction at the cathode of REDR.
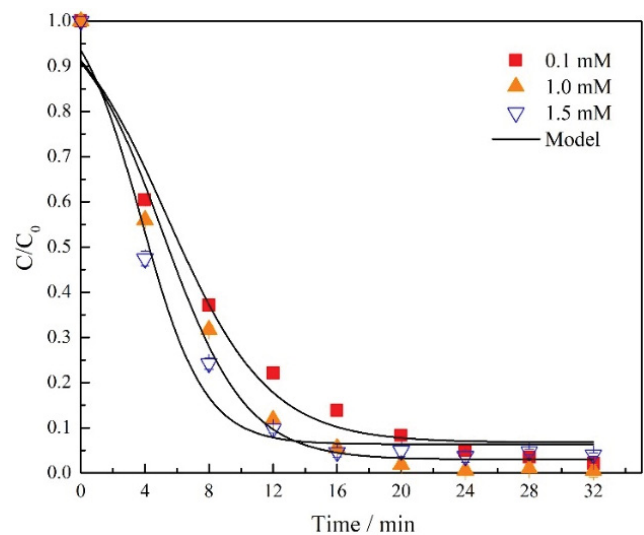

Fig. 4. Effect of Fe^{2+} concentration on decolorization efficiency of MO simulative wastewater in the cathodic degradation loop (Operation conditions: pH value, CRS and airflow rate are 2, 82 and 800 mL min^{-1}, respectively). Curves connecting the points are fitted by a modified kinetic equation for the cathodic degradation loop [Eq. (20)], and the coefficients are given in Table 6.

Table 5
Kinetic parameters obtained after regression of the MO concentration histories for the anodic degradation loop

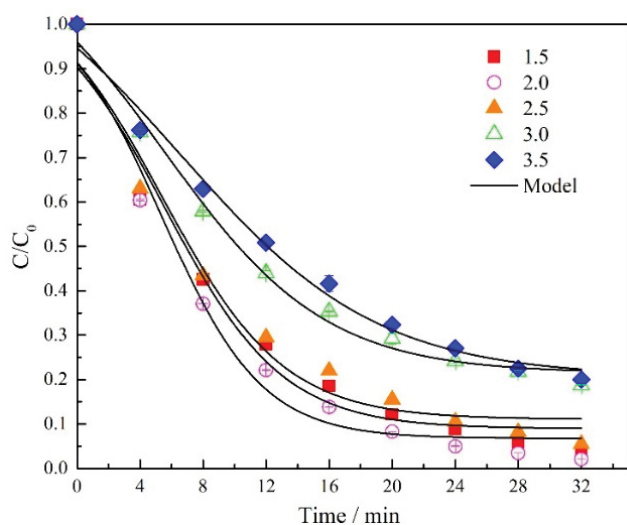| Operation parameter	unit	value	k (min^{-1})	t^* (min)	R^2
Chloride concentration	mol L^{-1}	0.05	0.59271	5.56449	0.99797
		0.1	0.65708	5.17953	0.99863
		0.3	0.93185	4.39997	0.9996
		0.5	0.88673	4.37257	0.9994
		32	0.53745	5.81392	0.99628
		56	0.55369	5.35519	0.99601
ARS flow rate	mL min^{-1}	82	0.88673	4.37257	0.9994
		108	1.06138	3.80181	0.99878
		128	1.43394	3.86181	0.99993

Fig. 5. Effect of pH value on decolorization efficiency of MO simulative wastewater in the cathodic degradation loop (Operation conditions: Fe^{2+} concentration, CRS and airflow rates are 0.1 mM, 82 and 800 mL min^{-1}, respectively). Curves connecting the points are fitted by a modified kinetic equation for the cathodic degradation loop [Eq. (20)], and the coefficients are given in Table 6.

- Under acidic condition, the H_2O_2 generated at the cathode is more easily decomposed into H_2O and O_2 as the pH value of wastewater increases.
- Ferrous ions combine more easily with OH$^-$ roots in wastewater to form hydroxide precipitation to lose its catalytic activity as the pH value of wastewater increases [31].

However, an extremely low pH value is also adverse to the decolorization efficiency. Under the condition of an extremely low pH value, a hydrogen evolution reaction and a reduction reaction of hydroxyl radical will occur at the cathode [32,33], which are expressed as follows:

$$2H^+ + 2e^- \rightarrow H_{2(g)} \tag{18}$$

$$^{\bullet}OH + H^+ + e^- \rightarrow H_2O \tag{19}$$

The experimental results (shown in Fig. 5) show that after treatment for 20 min, the decolorization efficiencies are 87.81%, 91.71%, 84.52%, 70.79% and 67.61% when the pH values of the wastewater are 1.5, 2, 2.5, 3 and 3.5, respectively. Under the given operation conditions, the decolorization efficiency is the highest when the pH value of the wastewater is 2.

3.2.3. Effect of airflow rate

The purpose of blowing air into the CRS is to increase the oxygen content in the wastewater, which can promote the reduction reaction at the cathode. A microporous aerator pipe set at the bottom of the carbon felt cathode in the cathode channel is used as a bubble generator. A tiny number of bubbles form in the CRS when the air is blown by an air pump. Therefore, variations in the airflow rate will influence the decolorization efficiency of wastewater. Fig. 6 shows the effect of the airflow rate on the decolorization efficiency of the wastewater.

Fig. 6 shows that the decolorization efficiency decreases with increasing airflow rate at the same treatment time. After treatment for 20 min, the decolorization efficiency decreased from 89.05% to 78.95%, with the airflow rate increasing from 400 to 1,200 mL min^{-1}. The reason is that more tiny air bubbles will assemble on the cathode surface to decrease the area in contact with the wastewater and electrode when the airflow rate is too large, which will impede the reduction and EF reactions at the cathode [34]. Therefore, the airflow rate of 400 mL min^{-1} is sufficient for reduction and EF reactions at the cathode in this experiment, and the decolorization efficiency drops when the airflow rate exceeds 400 mL min^{-1}.

3.2.4. Effect of CRS flow rate

Fig. 7 illustrates the effect of the CRS flow rate on the decolorization efficiency of the wastewater. It can be seen from the figure that the decolorization efficiency decreases with increasing CRS flow rate at the same treatment time. After treatment for 20 min, the decolorization efficiency increased from 54.32% to 98.42%, with the CRS flow rate rising from 32 to 128 mL min^{-1}.

By comparing Fig. 3 with Fig. 7, it can be found that the variation in the ERS flow rate affects the decolorization efficiency in both degradation loops. Nevertheless, the influence of CRS flow rate variation on the decolorization efficiency is greater than that of ARS flow rate variation on the decolorization efficiency. The reasons are as following:

- Because the thickness of the cathodic channel is larger than that of the anodic channel, the effect of CRS flow rate variation on oxidant diffusion in the cathodic channel is greater than that in the anodic channel.
- Since the strong oxidant hydroxyl radical has a nonselective and short lifetime (estimated as only a few nanoseconds in water), an increase in the CRS flow rate can enhance the contact opportunity between the oxidant and organic pollutants in wastewater.
- Since Fe^{2+} affects the EF reaction, increasing the CRS flow rate means that more ferrous ions and organic pollutants pass through the cathodic channel per unit time, which is beneficial to the cathodic degradation process.

Table 6 lists all experimental conditions of the cathodic degradation loop and the kinetic parameters obtained after the regression of MO concentration histories in the wastewater. It can be seen from the table that there is a better fit precision between the experimental data and the data calculated by a modified kinetic equation [Eq. (20)].

3.3. Effect of current density

The current density is an essential working parameter in the electrochemical degradation process of REDRs, and
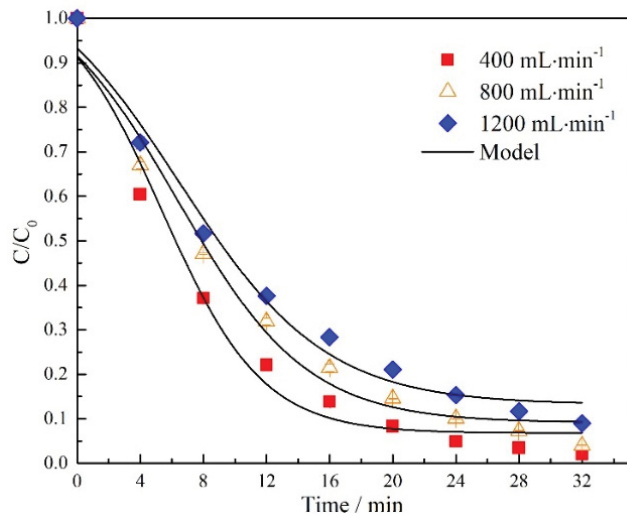
Fig. 6. Effect of airflow rate on decolorization efficiency of MO simulative wastewater in the cathodic degradation loop (Operation conditions: Fe^{2+} concentration, pH value and CRS flow rate are 0.1 mM, 2 and 82 mL min^{-1}, respectively). Curves connecting the points are fitted by a modified kinetic equation for the cathodic degradation loop [Eq. (20)], and the coefficients are given in Table 6.

Fig. 7. Effect of CRS flow rate on decolorization of MO simulative wastewater in the cathodic degradation loop (Operation conditions: Fe^{2+} concentration, pH value and airflow rate are 0.1 mM, 2 and 800 mL min^{-1}, respectively). Curves connecting the points are fitted by a modified kinetic equation for the cathodic degradation loop [Eq. (20)], and the coefficients are given in Table 6.
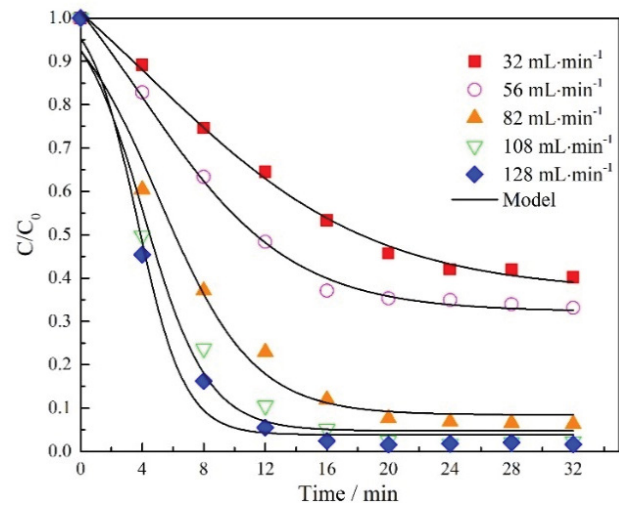
it plays an important role in the decolorization efficiency of the wastewater in the two loops. Fig. 8 shows the effect of current density on the decolorization efficiencies of the wastewater. All operating conditions in the two loops are unchanged during experiments, and only the current density or current changes.

Fig. 8 illustrates that at the same treatment time, the decolorization efficiencies of the wastewater rise in both the anodic and cathodic degradation loops as the current density increases. However, it can be found by comparing Fig. 8A with Fig. 8B that accept the conditions of a small current density and short treatment time, the decolorization efficiencies of the wastewater in the anodic degradation loop are always higher than those in the cathodic degradation loop. When the current density increases from 0.62 to 3.10 A m^{-2}, after treating for 8 min, the decolorization efficiency of the wastewater in the anodic degradation loop rises from 19.80% to 95.05%, but that in the cathodic degradation loop rises

Table 6
Kinetic parameters obtained after regression of the MO concentration histories for the cathodic degradation loop

| Operation parameter	unit	value	k (min^{-1})	t^* (min)	C_{ec} (mg L^{-1})	R^2
		0.1	0.31478	5.37569	6.764	0.97008
Ferrous concentration	mmol L^{-1}	1.0	0.40749	459833	6.500	0.97015
		1.5	0.50832	3.75622	6.334	0.9749
		1.5	0.26646	5.5339	8.963	0.96146
		2	0.31478	5.37569	6.764	0.97008
pH value	/	2.5	0.25942	5.43199	11.000	0.96927
		3	0.19478	5.51993	21.457	0.98896
		3.5	0.15929	6.57978	20.632	0.98401
		600	0.31478	5.37569	6.764	0.97008
Airflow rate	mL min^{-1}	800	0.24317	6.36785	9.11	0.97285
		1,200	0.21596	6.46449	13.19	0.97851
		32	0.13607	4.38373	36.765	0.99569
		56	0.20579	3.90084	32.299	0.996
CRS flow rate	mL min^{-1}	82	0.31478	5.37569	6.764	0.97008
		108	0.48138	4.0968	4.771	0.97502
		128	0.64748	3.65918	3.836	0.98545
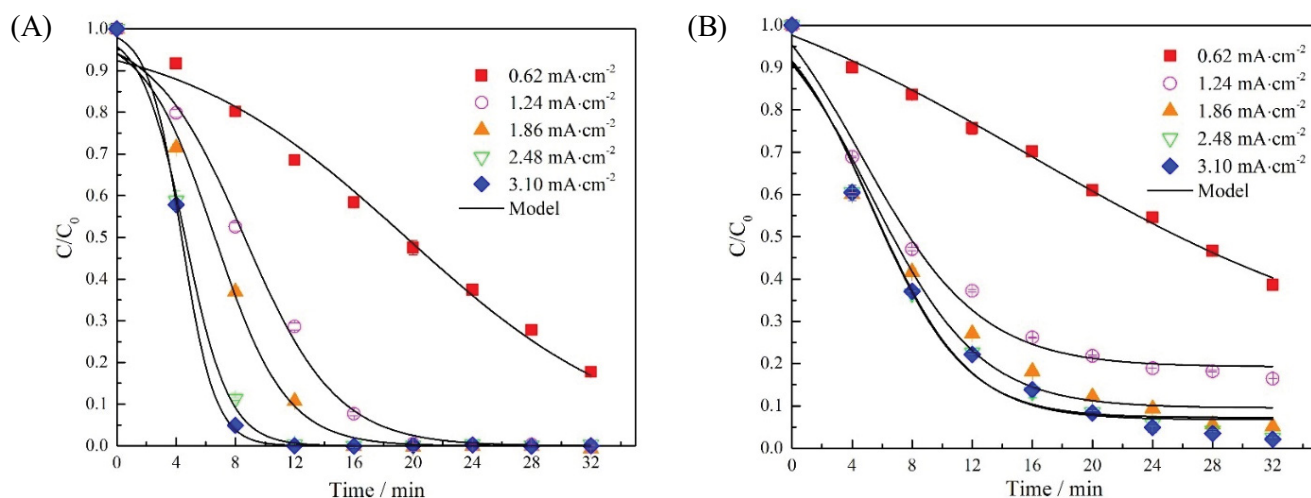
Fig. 8. Effect of current density on decolorization efficiency of MO simulative wastewater in the anodic degradation loop (A), and the cathodic degradation loop (B) (Operation conditions: ARS, chloride concentration and ARS flow rate are 0.5 M and 82 mL min^{-1}; CRS, Fe^{2+} concentration, pH value, air and CRS flow rates are 0.1 mM, 2, 800 and 82 mL min^{-1}). Curves connecting the points are fitted by Eqs. (17) and (20), respectively, and the coefficients are given in Table 7.

from 16.5% to 62.9%. This is because the oxidation process of the EF method includes several processes, and enhancing the current density only increases the reaction rate of the first step. Therefore, the argument of current density promotes decolorization efficiency for anodic degradation loop more than cathodic degradation loop.

It can also be seen from Fig. 8 that the effect of current density variation on the decolorization efficiency is greater when the current density is relatively smaller. Nevertheless, the effect of current density variation on the decolorization efficiency is less when the current density is relatively larger. When the current density rises from 0.62 to 1.24 A m^{-2}, after treating for 8 min, the decolorization efficiency rises from 19.80% to 47.50% as the anodic degradation loop increases by 239.89%. Moreover, it rises from 16.51% to 53.02% in the cathodic degradation loop, increasing by 321.14%. However, at the same treatment time, when the current density rises from 2.48 and 3.10 A m^{-2}, the decolorization efficiency rises from 88.75% to 95.05% in the anodic degradation loop and only increases by 10.7%. Furthermore, they are almost the same (from 63.49% to 62.28%) in the cathodic degradation loop (the experimental data almost overlap). The results indicate that the current efficiency of the wastewater process drops as the current density increases. The reason is that some side reactions at the electrodes will be created at a high current density, which will reduce the electron transfer efficiency at the electrodes. Moreover, the side reactions react with hydroxyl radical to reduce the decolorization efficiency of the wastewater [35,36].

Table 7 lists all experimental conditions of current density and kinetic parameters obtained after regression of the MO concentration histories in the wastewater in the two loops. It can be seen from the table that there is a better fit precision between the experimental data and the data calculated by Eq. (17) for the anodic degradation loop and by a modified kinetic equation [Eq. (20)] for the cathodic degradation loop.

3.4. Kinetic model for the degradation loop

The kinetic model, based on Fermi's equation as shown in Eq. 17, was developed earlier and applied here to demonstrate the concentration histories of MO. This model is used to explain the influence of the working conditions on the decoloration efficiency of MO in two degradation loops. The fittings for the different operating conditions are shown in Figs. 2–8, and the kinetic model presents an inverse S-shaped profile curve by fitting the results data. The relevant model parameters under different conditions obtained after regression are also summarized in Tables 5–7.

In Tables 5–7, the value of k presents a similar variation trend with decoloration efficiency in the above section, and the value of t^* is in contrast. The reason is that the apparent rate constant k from the kinetic model fitting reflects the MO degradation rate. Therefore, the variation in k can also be explained by the discussion results in Section 3.1–3.3. Meanwhile, the transition time t^* is related to the oxidant accumulation in the reaction compartment. Therefore, the more rapid the rate of oxidant generation, the shorter the transition time. Furthermore, it can also be found by comparing Tables 5–7. The effect of current density variation on the reaction rate (k) and transition time (t^*) is more significant than the operation condition variation. This phenomenon indicated that increasing the current density could speed up the electro-generation oxidant, and its promotion was superior to other conditions.

It can be seen from Table 5 that for the anodic degradation loop, the fitting precisions, R^2 values, are in the ranges of 0.981 to 0.999. This means that the model is in good agreement with the experimental data. However, the fitted results by Eq. (17) are not better coincident with the experimental data for the cathodic degradation loop. The reason is that a flocculant, Fe(OH)$_2$, can be generated by combining Fe^{2+} and O$_2$ due to an electrocoagulation phenomenon in a narrow cathodic channel of REDR [37,38]. The MO dye in the

Table 7
Kinetic parameters obtained after regression of the MO concentration histories for the two loops

Current density (A m^{-2})	Anodic degradation loop			Cathodic degradation loop			
	k (min^{-1})	t^* (min)	R^2	k (min^{-1})	t^* (min)	C_{ec} (mg L^{-1})	R^2
0.62	0.12782	19.5334	0.98179	0.08158	15.8945	19.097	0.99298
1.24	0.32262	8.61848	0.99425	0.2519	4.60178	19.23	0.98403
1.86	0.41815	6.61662	0.99453	0.27611	5.30423	9.538	0.96289
2.48	0.67746	4.61179	0.99729	0.31901	5.27672	7.225	0.97155
3.1	0.88673	4.37257	0.9994	0.31478	5.37569	6.764	0.97008

wastewater combined with Fe(OH)$_2$ will be sorbed on the carbon felt surface to reduce the efficient reaction area of the electrode, which will decrease the decolorization efficiency. Nevertheless, the electrocoagulation phenomenon will be weakened with increasing CRS flow rate and current density. Therefore, a coefficient of electrocoagulation, C_{ec}, is introduced into Fermi's function for the cathodic degradation loop of REDR, and the kinetic model is modified as follows:

$$\frac{C_{cathode}}{C_0} = \frac{1}{1+\exp\left[k\left(t-t^*\right)\right]} + \frac{C_{ec}}{C_0} \quad (20)$$

where C_{ec} represents the variation of dye concentration due to the electrocoagulation phenomenon, mg L^{-1}.

From Table 6, the modified model presents good agreement with the experimental data due to the high value of R^2. Eq. (20) indicates that a high C_{ec} value means a low decolorization efficiency at the same treatment time. Tables 6 and 7 show that within the range of experimental parameter variations, the values of C_{ec} decrease with the CRS flow rate and the current density increasing. The reasons are that 1) the turbulence of CRS in the cathodic channel will promote as the flow rate increases, which leads to the flocculant not easily sorbed by the carbon felt electrode; 2) the reduction and EF reactions at the cathode will boost as the current density increases, which leads to the enlargement of Fe^{2+} consumption and the flocculant not easily formed. It can also be found from Table 6 that the influences of Fe^{2+} concentration and pH value increases on the value of C_{ec} express a trend of fall first and rise later, but the value of C_{ec} rises with the increase of airflow rate.

3.5. Comparison of other treatment methods

Many reports about azo dye wastewater treatment methods have been proposed. Ramírez et al. [39] used two compartments of an electrochemical reactor to degrade azo dyes simultaneously. The results indicate that azo dye could be degraded simultaneously in both chambers of the electrochemical reactor. Meanwhile, the removal efficiency of azo dye can reach 99% during the first 100 min of electrolysis. The removal efficiency of 76% can be achieved in an anolyte at the end of the treatment. Ramírez et al. [40] also reported relevant research on advanced indirect oxidation of Acid Orange 7 (AO7) using an unmodified carbon

fabric cathode. It was found that the oxidation process of AO7 indirect oxidation (in the concentration range of 0.12–0.24 mM) by Fenton chemistry follows a first-order kinetic equation. Moreover, the energy required for 0.24 mM AO7 degradation is 1.04 kWh m^{-3}. Li et al. [41] reported another wastewater treatment process of electrochemistry synergetic with granulated activated carbon catalysis of peroxymonosulfate (electro/GAC/PMS) to degrade AO7 wastewater. The results show that the decolorization efficiency of AO7 reached 93.9% for 250 mL of AO7 wastewater at 100 mg L^{-1} after electrolytic treatment for 60 min, and the PMS was decomposed in the oxidation process.

Compared to the above organic wastewater treatment technologies, the advantages of the novel treatment method by REDR are (1) two oxidation processes in two electrode compartments of REDR are adopted to degrade organics and can obtain a high decoloration efficiency; (2) the energy consumption mainly comes from salt gradient energy between working solutions and does not require external electrical energy; (3) no other reactant dosage is needed.

4. Conclusions

The decolorization efficiencies of MO simulative wastewater by REDR under different operation conditions were investigated by experiments in this work. The influence of operation condition variations on the decolorization efficiencies in the two degradation loops was analyzed and discussed. Meanwhile, a semi-empirical kinetic model based on Fermi's equation was introduced into this work to describe the MO concentration histories obtained in the parametric study. The conclusions are helpful for 'waste-heat to treat wastewater' technology and can be drawn as follows:

- The color of MO simulative wastewater in the two degradation loops could be effectively faded by REDR. Except for the conditions of a small current density and short treatment time, the decolorization efficiency of the anodic degradation loop was superior to that of the cathodic degradation loop under the given conditions.
- The variations in the ERS flow rate and current density had a more significant influence than other operation parameters on the decolorization efficiency of the wastewater in the two loops. Meanwhile, the pH value of the wastewater also played an important role in the decolorization efficiency in the cathodic degradation loop, and its optimal value was 2.

- The kinetic model based on Fermi's equation had a good fit for the experimental data of the anodic degradation loop. However, the model should be modified to fit the experimental data of the cathodic degradation loop because of an electrocoagulation phenomenon. After a correction term was added to the conventional kinetic model, the modified model had a good fit for the experimental data of the cathodic degradation loop.

Conflict of interest

The authors declare that there are no known competing financial interests or personal relationships that could have appeared to influence the work reported in this paper.

Acknowledgement

References

[1] D.A. Yaseen, M. Scholz, Textile dye wastewater characteristics and constituents of synthetic effluents: a critical review, Int. J. Environ. Sci. Technol., 16 (2019) 1193–1226.

[2] A. Rahmani, M. Leili, A. Seid-Mohammadi, A. Shabanloo, A. Ansari, D. Nematollahi, S. Alizadeh, Improved degradation of diuron herbicide and pesticide wastewater treatment in a three-dimensional electrochemical reactor equipped with PbO_2 anodes and granular activated carbon particle electrodes, J. Cleaner Prod., 322 (2021) 129094, doi: 10.1016/j.jclepro.2021.129094.

[3] M.R. Samarghandi, A. Dargahi, A. Rahmani, A. Shabanloo, A. Ansari, D. Nematollahi, Application of a fluidized three-dimensional electrochemical reactor with Ti/SnO_2–Sb/β-PbO_2 anode and granular activated carbon particles for degradation and mineralization of 2,4-dichlorophenol: process optimization and degradation pathway, Chemosphere, 279 (2021) 130640, doi: 10.1016/j.chemosphere.2021.130640.

[4] F.C. Moreira, R.A.R. Boaventura, E. Brillas, V.J.P. Vilar, Electrochemical advanced oxidation processes: a review on their application to synthetic and real wastewaters, Appl. Catal., B, 202 (2017) 217–261.

[5] S. Garcia-Segura, J.D. Ocon, M.N. Chong, Electrochemical oxidation remediation of real wastewater effluents — a review, Process Saf. Environ. Prot., 113 (2018) 48–67.

[6] E. Brillas, I. Sirés, M.A. Oturan, Electro-Fenton process and related electrochemical technologies based on Fenton's reaction chemistry, Chem. Rev., 109 (2009) 6570–6631.

[7] P. Palenzuela, M. Micari, B. Ortega-Delgado, F. Giacalone, G. Zaragoza, D.C. Alarcón-Padilla, A. Cipollina, A. Tamburini, G. Micale, Performance analysis of a RED-MED salinity gradient heat engine, Energies, 11 (2018) 3385, doi: 10.3390/en11123385.

[8] R. Long, B. Li, Z. Liu, W. Liu, Hybrid membrane distillation-reverse electrodialysis electricity generation system to harvest low-grade thermal energy, J. Membr. Sci., 525 (2017) 107–115.

[9] X. Luo, X. Cao, Y. Mo, K. Xiao, X. Zhang, P. Liang, X. Huang, Power generation by coupling reverse electrodialysis and ammonium bicarbonate: implication for recovery of waste heat, Electrochem. Commun., 19 (2012) 25–28.

[10] S. Xu, Q. Leng, D. Jin, X. Wu, Z. Xu, P. Wang, D. Wu, F. Dong, Experimental investigation on dye wastewater treatment with reverse electrodialysis reactor powered by salinity gradient energy, Desalination, 495 (2020) 114541, doi: 10.1016/j.desal.2020.114541.

[11] S. Xu, Q. Leng, X. Wu, Z. Xu, J. Hu, D. Wu, D. Jing, P. Wang, F. Dong, Influence of output current on decolorization efficiency

[12] P.F. Ma, X.G. Hao, A. Galia, O. Scialdone, Development of a process for the treatment of synthetic wastewater without energy inputs using the salinity gradient of wastewaters and a reverse electrodialysis stack, Chemosphere, 248 (2020) 125994, doi: 10.1016/j.chemosphere.2020.125994.

[13] F. Zhang, S. Xu, D. Feng, S. Chen, R. Du, C. Su, B. Shen, A low-temperature multi-effect desalination system powered by the cooling water of a diesel engine, Desalination, 404 (2017) 112–120.

[14] D. González, J. Amigo, F. Suárez, Membrane distillation: perspectives for sustainable and improved desalination, Renewable Sustainable Energy Rev., 80 (2017) 238–259.

[15] J. Wang, S. Chen, X. Mu, S. Shen, Thermodynamic analysis of multistage flash distillation application in wastewater treatment, Int. J. Energy Clean Environ., 19 (2018) 85–91.

[16] O. Scialdone, A. D'Angelo, E. De Lumè, A. Galia, Cathodic reduction of hexavalent chromium coupled with electricity generation achieved by reverse-electrodialysis processes using salinity gradients, Electrochim. Acta, 137 (2014) 258–265.

[17] O. Scialdone, A. D'Angelo, A. Galia, Energy generation and abatement of Acid Orange 7 in reverse electrodialysis cells using salinity gradients, J. Electroanal. Chem., 738 (2015) 61–68.

[18] Y. Zhou, K. Zhao, C. Hu, H. Liu, Y. Wang, J. Qu, Electrochemical oxidation of ammonia accompanied with electricity generation based on reverse electrodialysis, Electrochim. Acta, 269 (2018) 128–135.

[19] M. Tedesco, A. Cipollina, A. Tamburini, I.D.L. Bogle, G. Micale, A simulation tool for analysis and design of reverse electrodialysis using concentrated brines, Chem. Eng. Res. Des., 93 (2015) 441–456.

[20] M. Panizza, G. Cerisola, Direct and mediated anodic oxidation of organic pollutants, Chem. Rev., 109 (2009) 6541–6569.

[21] E.B. Cavalcanti, S. Garcia-Segura, F. Centellas, E. Brillas, Electrochemical incineration of omeprazole in neutral aqueous medium using a platinum or boron-doped diamond anode: degradation kinetics and oxidation products, Water Res., 47 (2013) 1803–1815.

[22] F. Zhang, C.P. Feng, W.Q. Li, J.G. Cui, Indirect electrochemical oxidation of dye wastewater containing Acid Orange 7 using Ti/RuO_2-Pt electrode, Int. J. Electrochem. Sci., 9 (2014) 943–954.

[23] O. Ganzenko, C. Trellu, N. Oturan, D. Huguenot, Y. Péchaud, E.D. van Hullebusch, M.A. Oturan, Electro-Fenton treatment of a complex pharmaceutical mixture: mineralization efficiency and biodegradability enhancement, Chemosphere, 253 (2020) 126659, doi: 10.1016/j.chemosphere.2020.126659.

[24] P.F. Ma, H.R. Ma, A. Galia, S. Sabatino, O. Scialdone, Reduction of oxygen to H_2O_2 at carbon felt cathode in undivided cells. Effect of the ratio between the anode and the cathode surfaces and of other operative parameters, Sep. Purif. Technol., 208 (2019) 116–122.

[25] J. Herney-Ramirez, A.M.T. Silva, M.A. Vicente, C.A. Costa, L.M. Madeira, Degradation of Acid Orange 7 using a saponite-based catalyst in wet hydrogen peroxide oxidation: kinetic study with the Fermi's equation, Appl. Catal., B, 101 (2011) 197–205.

[26] D. Ghime, P. Ghosh, Decolorization of diazo dye trypan blue by electrochemical oxidation: kinetics with a model based on the Fermi's equation, J. Environ. Chem. Eng., 8 (2020) 102792, doi: 10.1016/j.jece.2018.11.037.

[27] L. Labiadh, A. Barbucci, M.P. Carpanese, A. Gadri, S. Ammar, M. Panizza, Comparative depollution of Methyl orange aqueous solutions by electrochemical incineration using $TiRuSnO_2$, BDD and PbO_2 as high oxidation power anodes, J. Electroanal. Chem., 766 (2016) 94–99.

[28] D. Gumus, F. Akbal, Comparison of Fenton and electro-Fenton processes for oxidation of phenol, Process Saf. Environ. Prot., 103 (2016) 252–258.

[29] M. Malakootian, A. Moridi, Efficiency of electro-Fenton process in removing Acid Red 18 dye from aqueous solutions, Process Saf. Environ. Prot., 111 (2017) 138–147.

[30] H. Lin, N. Oturan, J. Wu, H. Zhang, M.A. Oturan, Cold incineration of sucralose in aqueous solution by electro-Fenton process, Sep. Purif. Technol., 173 (2017) 218–225.

[31] V. Khandegar, A.K. Saroha, Electrocoagulation for the treatment of textile industry effluent – a review, J. Environ. Manage., 128 (2013) 949–963.

[32] N. Wang, T. Zheng, G. Zhang, P. Wang, A review on Fenton-like processes for organic wastewater treatment, J. Environ. Chem. Eng., 4 (2016) 762–787.

[33] Q. Lei, B.G. Wang, P.C. Wang, S. Liu, Hydrogen generation with acid/alkaline amphoteric water electrolysis, J. Energy Chem., 38 (2019) 162–169.

[34] S. Qiu, D. He, J.X. Ma, T.X. Liu, T.D. Waite, Kinetic modeling of the electro-fenton process: quantification of reactive oxygen species generation, Electrochim. Acta, 176 (2015) 51–58.

[35] H.Q. He, Z. Zhou, Electro-Fenton process for water and wastewater treatment, Crit. Rev. Env. Sci. Technol., 47 (2017) 2100–2131.

[36] B. Hou, H. Han, S. Jia, H. Zhuang, P. Xu, K. Li, Three-dimensional heterogeneous electro-Fenton oxidation of biologically pretreated coal gasification wastewater using sludge derived carbon as catalytic particle electrodes and catalyst, J. Taiwan Inst. Chem. Eng., 60 (2016) 352–360.

[37] Z. Yi, C. Yanqing, S.U.N. Peide, Experiment and kinetic model for Methyl orange wastewater removal by electrocoagulation, Huagong Xuebao (Chin. Ed.), 60 (2009) 2339–2345.

[38] S.Y. Lee, G.A. Gagnon, Growth and structure of flocs following electrocoagulation, Sep. Purif. Technol., 163 (2016) 162–168.

[39] B. Ramirez-Pereda, A.A. Alvarez-Gallegos, S. Silva-Martinez, J.G. Rangel-Peraza, Y.A. Bustos-Terrones, Evaluation of the simultaneous use of two compartments of an electrochemical reactor for the elimination of azo dyes, J. Electroanal. Chem., 855 (2019) 113593, doi: 10.1016/j.jelechem.2019.113593.

[40] B. Ramirez, V. Rondan, L. Ortiz-Hernandez, S. Silva-Martinez, A. Alvarez-Gallegos, Semi-empirical chemical model for indirect advanced oxidation of Acid Orange 7 using an unmodified carbon fabric cathode for H_2O_2 production in an electrochemical reactor, J. Environ. Manage., 171 (2016) 29–34.

[41] J. Li, H. Lin, K. Zhu, H. Zhang, Degradation of Acid Orange 7 using peroxymonosulfate catalyzed by granulated activated carbon and enhanced by electrolysis, Chemosphere, 188 (2017) 139–147.